Extracellular matrix protein βig-h3/TGFBI promotes metastasis of colon cancer by enhancing cell extravasation

Chaoyu Ma,[1] Yu Rong,[1] Daniel R. Radiloff,[1] Michael B. Datto,[2] Barbara Centeno,[3] Shideng Bao,[4] Anthony Wai Ming Cheng,[2] Fumin Lin,[1] Shibo Jiang,[5] Timothy J. Yeatman,[3] and Xiao-Fan Wang[1,6]

[1]Department of Pharmacology and Cancer Biology, Duke University Medical Center, Durham, North Carolina 27710, USA; [2]Department of Pathology, Duke University Medical Center, Durham, North Carolina 27710, USA; [3]Department of Surgery, H. Lee Moffitt Cancer Center and Research Institute, Tampa, Florida 33612, USA; [4]Department of Radiation Oncology and Department of Neurosurgery, University of Colorado at Denver and Health Science Center, Aurora, Colorado 80045, USA; [5]Lindsley F. Kimball Research Institute, New York Blood Center, New York, New York 10021, USA

Metastasis, the major cause of cancer death, is a multistep process that requires interactions between cancer cells and stromal cells and between cancer cells and extracellular matrix. Molecular alterations of the extracellular matrix in the tumor microenvironment have a considerable impact on the metastatic process during tumorigenesis. Here we report that elevated expression of βig-h3/TGFBI (transforming growth factor, β-induced), an extracellular matrix protein secreted by colon cancer cells, is associated with high-grade human colon cancers. Ectopic expression of the βig-h3 protein enhanced the aggressiveness and altered the metastatic properties of colon cancer cells in vivo. Inhibition of βig-h3 expression dramatically reduced metastasis. Mechanistically, βig-h3 appears to promote extravasation, a critical step in the metastatic dissemination of cancer cells, by inducing the dissociation of VE-cadherin junctions between endothelial cells via activation of the integrin $\alpha_v\beta_5$–Src signaling pathway. Thus, cancers associated with overexpression of βig-h3 may have an increased metastatic potential, leading to poor prognosis in cancer patients.

Tumor metastasis consists of a series of complex steps, all of which must be successfully completed to give rise to clinically detectable metastatic tumors at distal organs (Woodhouse et al. 1997; Hanahan and Weinberg 2000; Chambers et al. 2002; Bierie and Moses 2006; Gomis et al. 2006). To complete the journey, primary cancer cells have to invade through the basement membrane, intravasate into the bloodstream, disseminate through the circulation, and extravasate to distal tissues/organs. The entire process, regulated by interactions between cancer cells and stromal cells and between cancer cells and extracellular matrix (ECM), remains poorly understood at the level of molecular mechanism.

Extravasation, the process by which tumor cells leave a blood or lymphatic vessel and invade the surrounding tissue parenchyma, requires dynamic interaction between cancer cells and endothelial cells lining the blood vessel wall (Weiss 1990; Chambers et al. 2002; MacDonald et al. 2002; Weis and Cheresh 2005). As a major component of the tumor microenvironment, ECM proteins secreted by cancer and/or stromal cells potentially affect the dissemination process through modulation of the interaction between cancer and endothelial cells (Bernstein and Liotta 1994). Recently, large-scale analyses of gene expression profiles of human cancers have revealed that aberrant expression patterns of ECM proteins are common among a wide range of cancer types (Buckhaults et al. 2001; Cooper et al. 2003), suggesting that alterations in the expression profiles of ECM proteins during tumor development can consequently exert a functional impact on the metastatic process, including extravasation (Gupta et al. 2007; Karnoub et al. 2007).

Previously we demonstrated that periostin, a secreted ECM protein that is overexpressed by several cancer types, promotes tumor angiogenesis and metastasis (Bao et al. 2004; Shao et al. 2004). βig-h3/*TGFBI* (transforming growth factor, β-induced; hereinafter referred to as βig-h3), a structural homolog of periostin, was found by se-

rial analysis of gene expression (SAGE) to be one of the genes that are highly elevated in various types of cancers (Zhang et al. 1997; Argani et al. 2001). βig-h3 contains an N-terminal secretory signal peptide, followed by a cysteine-rich domain, four internal homologous repeats (FAS1 domain), and a C-terminal RGD motif (Supplemental Fig. S1; Skonier et al. 1992). The FAS1 domain of βig-h3 shares high homology with fasciclin I, an axon guidance protein that is involved in neural development in invertebrates (Bastiani et al. 1987). Normally, the expression of βig-h3 is mainly found in fibroblasts, keratinocytes, and muscle cells (LeBaron et al. 1995; Bae et al. 2002; Ferguson et al. 2003). The physiological function of βig-h3 has been postulated to be involved in cell–matrix interaction and cell migration (Bae et al. 2002; Kim et al. 2003), and βig-h3 overexpression has been associated with atherosclerotic and restenotic vascular lesions in humans (O'Brien et al. 1996; Lee et al. 2006). In this report, we demonstrate that acquired expression of βig-h3 by colon cancer cells leads to a more aggressive phenotype of metastasis. βig-h3 induces the dissociation of VE-cadherin junctions between endothelial cells via the integrin $\alpha_v\beta_5$–Src signaling pathway, which results in enhanced cancer cell extravasation.

Results

βig-h3 expression is up-regulated in human colon cancers

Previous studies using the SAGE strategy have revealed that *TGFBI* expression is substantially elevated in colon and pancreatic cancers in comparison with corresponding normal tissues (representative results are summarized in Supplemental Table S1). Several subsequent studies using gene array analyses have also demonstrated that *TGFBI* is overexpressed in a majority of tumor samples in comparison with their normal tissue counterparts in colorectal cancer patients (summarized in Supplemental Table S2). To further confirm the association between human colon cancer and βig-h3 overexpression, we conducted a survey of βig-h3 expression using immunohistochemical staining of tissue microarray (TMA) samples derived from the colon tissue of 66 patients. βig-h3 overexpression was more frequent in high-grade (Stage III and IV) tumors (32.2%, *n* = 31) than in low-grade (Stage I and II) tumors (18.5%, *n* = 27), whereas no βig-h3 expression was detected in the normal epithelial tissues (*n* = 8) (Fig. 1A,B). Furthermore, βig-h3 overexpression is closely correlated with high-grade tumors derived from patients who were metastatic-prone or had already developed metastatic disease, indicating that high levels of βig-h3 may be associated with the metastatic process. (Information on patients from whom tumor samples were found with high expression levels of βig-h3 protein is summarized in Supplemental Tables S3, S4.)

### Overexpression of βig-h3 in colon cancer cells promotes tumor metastasis in vivo

To study the functional role of βig-h3 overexpression in colon cancer development, we used a model system con-sisting of two colon cancer cell lines, SW480 and SW620, derived from the primary tumor and lymph node metastasis of the same patient, respectively (Leibovitz et al. 1976). Previous studies with xenograft tumor growth in immunocompromised mice showed that the primary tumor-derived SW480 cell line exhibits a limited metastatic potential, whereas the lymph node metastasis-derived SW620 cell line displays an aggressive metastatic pattern (Hewitt et al. 2000). Importantly to this study, the two cell lines exhibit a different βig-h3 expression profile (Fig. 1C). To determine whether the difference in βig-h3 expression might be one of the reasons underlying the different metastatic potentials of this isogenic pair of cell lines, we stably expressed βig-h3 in the poorly metastatic SW480 cells to a level comparable with that of the aggressively metastatic SW620 cells (Fig. 1C). Equal numbers of SW480-βig-h3 or SW480-VEC control cells were then injected intravenously via the tail vein into 20 SCID-Beige mice, respectively. Twelve weeks after inoculation of the tumor cells, mice were sacrificed and examined for metastases in the lung and other organs. As shown in Figure 1, D and E, metastatic growth was easily detected in the lungs of all 20 mice injected with SW480-βig-h3 cells. A majority of these animals bore large numbers of tumors covering almost the entire lung. In contrast, only nine out of 20 mice injected with the SW480-VEC cells developed a small number of tumor nodules in the lung (Fig. 1D,E). The average number of visible metastatic nodules increased from 1.6 ± 2.1 per lung in mice carrying SW480-VEC control tumors to 23.2 ± 11.6 per lung in mice carrying SW480-βig-h3 tumors. Ectopic βig-h3 expression remained present in the metastatic tumors, which was confirmed by immunohistochemical staining (Fig. 1F). Interestingly, however, there was no significant difference in the average size of the metastatic tumors derived from the SW480-βig-h3 and SW480-VEC cells (Supplemental Fig. S2A; Supplemental Table S5). This suggests that βig-h3 expression in the SW480 cells significantly increased the probability of metastatic colonization in the lung without affecting the growth rate of metastasized tumors. Overall, our data suggest that βig-h3 overexpression is sufficient to promote the metastatic potential of colon cancer cell line SW480 in vivo.

Suppression of βig-h3 expression in SW620 cells significantly decreases their metastatic potential in vivo

We next performed loss-of-function experiments to test whether βig-h3 expression is required for the metastatic potential of the aggressive isogenic line of SW620 cells. We designed two shRNA sequences targeting different coding regions of the βig-h3 gene. Stable expression of the shRNA constructs considerably reduced the expression level of βig-h3 protein in the populations of SW620 cells (Fig. 2A). Equal numbers of the shRNA-expressing or vector-control SW620 cells were each intravenously injected into SCID-Beige mice via the tail vein. Seven weeks after inoculation, the SW620-VEC control cells formed a large number of tumor nodules in the lung (Fig.

Figure 1. Elevated βig-h3 expression is associated with high-grade colon cancers and an impact on metastasis of colon cancer cells. (*A*) Immunohistochemical analysis of βig-h3 expression in colon cancers. The tissue sections were immunostained with an anti-βig-h3 polyclonal antibody. The positive staining for βig-h3 protein is shown in a reddish-brown color. All sections were counterstained with hematoxylin showing a blue color. (Panel *a*) Normal colon mucosa (N), stroma (S), and epithelia (E). (Panel *b*) Adenomatous polyps (AP). (Panel *c*) Stage II colon adenocarcinoma (T II). (Panel *d*) Stage IV poorly differentiated colon adenocarcinoma (T IV). (*B*) The percentage of tissue samples with βig-h3 protein overexpression was plotted according to the malignant stage of the patient. Statistical analysis indicated that the high-grade tumors have a significantly higher ratio to associate with βig-h3 overexpression as compared with low-grade tumors ([*] $P = 0.026$) and normal tissues ([**] $P = 0.0035$). (*C*) Expression pattern of βig-h3 in SW480 and SW620 cells. SW480 cells (parental) were infected with recombinant retroviruses containing either vector control (VEC) or βig-h3 full-length cDNA tagged with the Flag-epitope (βig-h3). An equal amount of concentrated supernatant from each cell type as indicated was examined for the presence of βig-h3 by Western blot using an anti-βig-h3 or anti-Flag antibody. The whole-cell lysate from each sample of cells from which the supernatant was collected for the determination of βig-h3 expression was blotted with anti-tubulin antibody for loading control. (*D*) Representative results showing the formation of metastases in the lung of mice injected with SW480-VEC cells (C1, C2) and SW480-βig-h3 cells (T1, T2). We injected 4×10^6 SW480-VEC or SW480-βig-h3 cells through the tail vein into 5-wk-old SCID-Beige mice with five mice for each group.

Mice were sacrificed and examined for the growth of metastatic tumors 12 wk after injection. Four independent experiments were performed. Arrows indicate metastatic tumors in the mouse lung. (*E*) Representative results from two independent experiments showing total numbers of lung metastatic nodules in individual mouse injected with SW480-VEC or SW480-βig-h3 cells. The counting was performed under a dissection scope. ([*] $P < 0.01$ [$n = 10$]). (*F*) Immunohistochemical staining with paraffin-embedded sections of lung tissues isolated from mice intravenously inoculated with SW480-VEC or SW480-βig-h3 cells. (Panels *a*,*c*) Paraffin-embedded sections stained for the presence of βig-h3 in tumors derived from SW480-VEC cells (panel *a*) and SW480-βig-h3 cells (panel *c*). Positive staining is depicted in brown color. (Panels *b*,*d*) Hematoxylin/eosin staining for sections derived from SW480-VEC cells (panel *b*) and SW480-βig-h3 cells (panel *d*). Arrows indicate tumors in the mouse lung.
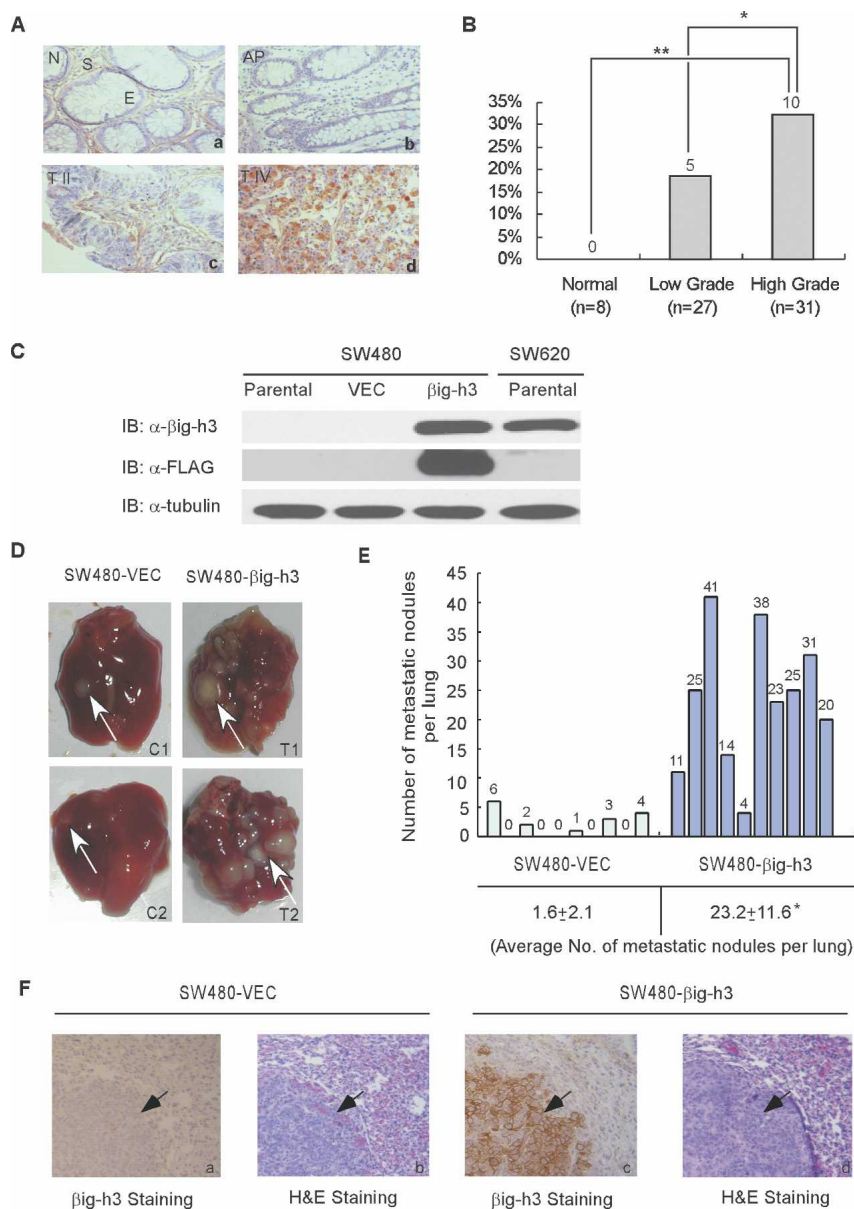
2C,D). In addition, the SW620-VEC control cells also formed tumor masses derived from lymph nodes around bilateral axillary and lateral thoracic regions, which had migrated to the back of the animals (Fig. 2B,D). In sharp contrast, the SW620-βig-h3-shRNA1 and SW620-βig-h3-shRNA2 cells showed significantly reduced lung and lymph node metastasis (Fig. 2B–D). Furthermore, all mice injected with SW620-VEC cells (10 of 10) also had

adrenal gland and mesentery metastasis, which was seen in only 20% (two of 10) of the mice injected with the βig-h3 knockdown cells (representative results are shown in Supplemental Fig. S3). Again, the average size of each metastatic tumor colony in the lung was comparable for the SW620-VEC and SW620-βig-h3-shRNA cells (Supplemental Fig. S2B; Supplemental Table S6), supporting the assumption that βig-h3 expression affects
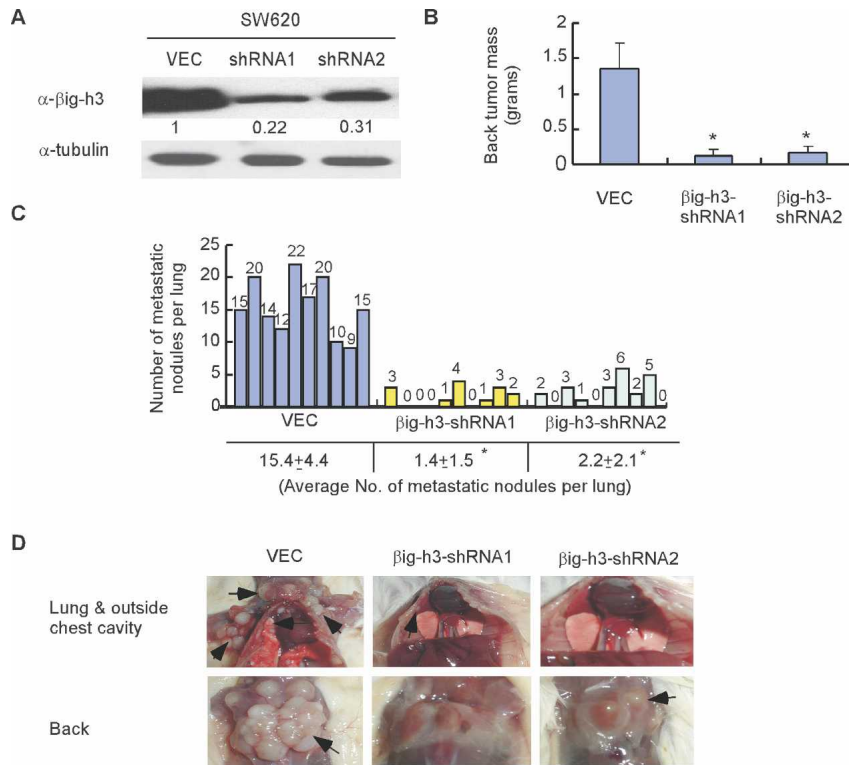
Figure 2. Reduction in the expression level of βig-h3 in SW620 colon cancer cells inhibits metastasis in vivo. (*A*) The expression level of βig-h3 in SW620 cells was reduced by 78% and 69%, respectively, using two different shRNA constructs. SW620 cells (parental) were infected with recombinant retroviruses containing vector control (VEC), shRNA1 (βig-h3-shRNA1), or shRNA2 (βig-h3-shRNA2). An equal amount of concentrated supernatant from each cell type as indicated was examined for the presence of βig-h3 by Western blot using an anti-βig-h3 antibody. The whole-cell lysate from each sample of cells from which the supernatant was collected for the determination of βig-h3 expression was blotted with anti-tubulin antibody for loading control. (*B*) Reduced βig-h3 expression led to decreases in tumor formation on the back of mice by the SW620 cells. We injected 2×10^6 SW620-VEC, SW620-βig-h3-shRNA1, or SW620-βig-h3-shRNA2 cells through the tail vein into 5-wk-old SCID-Beige mice with five animals for each group. Mice were sacrificed and examined for the growth of metastatic tumors 7 wk after injection. Results are the mean ± SD of five animals from each group. Four independent experiments were performed. (*) $P < 0.01$ ($n = 5$). (*C*) Representative results from two independent experiments showing total numbers of lung metastatic nodules in individual mouse injected with SW620-VEC, SW620-βig-h3-shRNA1, or SW620-βig-h3-shRNA2 cells. The counting was performed under the dissection scope. (*) $P < 0.01$ ($n = 10$). (*D*) Representative results showing that injection of SW620-VEC cells or SW620-βig-h3-shRNA1 and SW620-βig-h3-shRNA2 via tail veins led to different patterns in the formation of metastatic tumors.

primarily the number of metastatic colonies without changing the size of each colony.

To validate these results, we conducted a rescue experiment to exclude any possibility of an off-target effect associated with the shRNA approach. An shRNA-resistant βig-h3 gene (βig-h3n) was expressed in SW620-shRNA1 cells to a level that was 1.67-fold higher than the endogenous level of βig-h3 in the parental SW620 cells transfected with a control vector (Fig. 3A). Surprisingly, merely 4 wk after tail vein injection, the SW620-βig-h3n cells were already detected inside the skull, in adrenal glands and the lymph nodes (Fig. 3B–E). At this time point, no tumor masses were detected in any of the mice inoculated with the control SW620-VEC cells, suggesting that a further increase in the level of βig-h3 expression in SW620 cells led to an even more aggressive metastatic phenotype. Together, all these data from the tail vein injection experiments strongly suggest that the level of βig-h3 expression dictates the aggressiveness of SW620 colon cancer cells.

To further confirm the role of βig-h3 in the metastatic process, we examined the tumor cell metastasis in mice following intracardiac injection (Yin et al. 1999). Consistent with the previous intravenous injection experiments, SW620 or SW480 cancer cells with higher levels of βig-h3 expression displayed a more aggressive behav-

ior in forming metastatic colonies in distal organs, such as adrenal gland, bone, and mesentery, when compared with their paired control tumor cells with lower levels of βig-h3 expression (Fig. 3F–H). Taken together, these results support the notion that βig-h3, when acquired or overexpressed, has a profound impact on the formation of tumor metastasis by the colon cancer cells.

βig-h3 promotes trans-endothelial cell migration (TEM) in vitro by inducing VE-cadherin junction dissociation in the endothelial monolayer

To explore the mechanism by which βig-h3 expression has an impact on metastasis, we performed a series of in vitro functional assays. In our previous studies, we showed that periostin enhances tumor metastasis by promoting both angiogenesis and cell survival (Bao et al. 2004; Shao et al. 2004). Since βig-h3 shares significant structural homology with periostin (Supplemental Fig. S1; Skonier et al. 1992; Horiuchi et al. 1999) and both proteins play positive roles in tumor metastatic progression, we examined if βig-h3 has the same effects on tumor cells. Unlike periostin, however, βig-h3 showed no effect on cell survival under hypoxic conditions and failed to rescue the anoikis-induced apoptosis of the cancer cells (Supplemental Fig. S4). On the other hand, blood
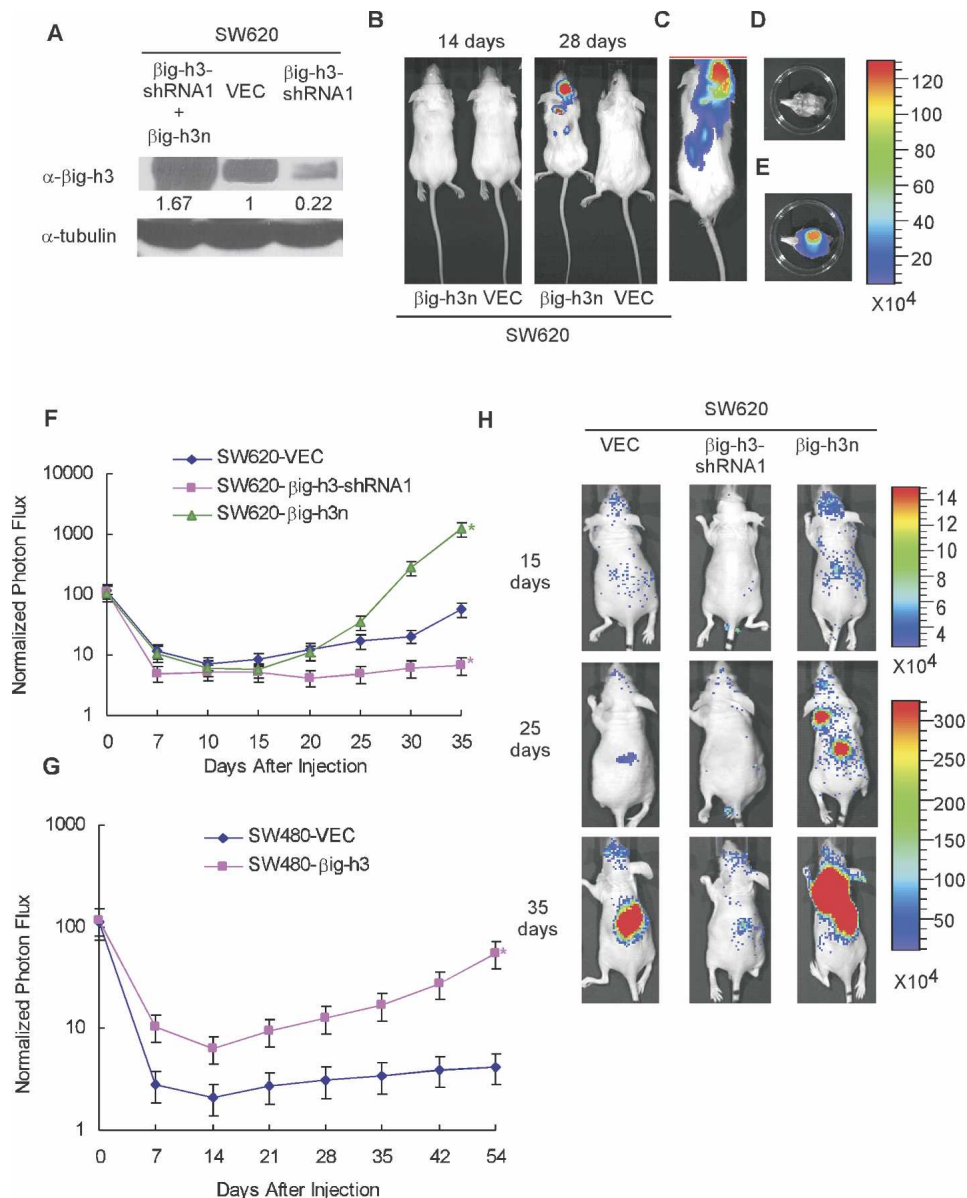
Figure 3. The metastatic properties of SW620 cells with different levels of βig-h3 expression. (*A*) The expression level of βig-h3 in SW620-βig-h3n, SW620-VEC, and SW620-βig-h3-shRNA1 cells. SW620-βig-h3-shRNA1 cells were infected with recombinant retroviruses containing shRNA-resistant βig-h3 full-length cDNA (βig-h3n) tagged with the Flag-epitope (SW620-βig-h3n). An equal amount of concentrated supernatant from each cell type as indicated was examined for the presence of βig-h3 by Western blot using an anti-βig-h3 antibody. The whole-cell lysate from each sample of cells from which the supernatant was collected for the determination of βig-h3 expression was blotted with anti-tubulin antibody for loading control. (*B*) Mice were injected intravenously with SW620-βig-h3n or SW620-VEC cells expressing a luciferase gene and subjected to in vivo imaging at indicated time points, with relative light unit counts indicated in color. (*C*) In vivo bioluminescent imaging of a mouse 4 wk after being inoculated with SW620-βig-h3n cells. (*D,E*) At necropsy, the skull (without brain tissue) of the same mouse shown in *C* was removed and imaged ex vivo for photographic (*D*) and bioluminescence (*E*) imaging. (*F,G*) SW620- and SW480-derived cells as indicated were inoculated intracardially into 5-wk-old nude mice. SW620 or SW480 cells were labeled with luciferase, and 1×10^6 cells were injected into the left cardiac ventricle of five mice for each group. At the indicated days after inoculation, bioluminescence images were acquired. Tumor metastasis was measured by bioluminescence and quantified. Results are the mean ± SD of five animals from each group. (*) $P < 0.05$. Two independent experiments were performed. (*H*) Representative in vivo bioluminescent images of animals after intracardiac inoculation. Representative mice from SW620-βig-h3n, SW620-VEC, and SW620-βig-h3-shRNA1 groups are shown in the prone position, with relative light unit counts indicated in color.

vessel density was similar in xenograft tumors derived from βig-h3-overexpressing and control cells, which sug-

gests that βig-h3 is not actively involved in the induction of angiogenesis (data not shown). Thus, although

highly homologous to periostin, βig-h3 promotes tumor metastasis through a distinct mechanism.

As mentioned earlier, the average size of metastatic lung tumor nodules was not affected by the different levels of βig-h3 expressed by the constituent cancer cells (Supplemental Fig. S2; Supplemental Tables S5, S6), indicating that βig-h3 expression may not function to accelerate cell proliferation. Consistent with this notion, ectopic βig-h3 expression only slightly enhanced subcutaneous tumor growth of the SW480 tumors (Supplemental Fig. S5A), and the proliferation rate of the SW480-VEC and SW480-βig-h3 cells was comparable (Supplemental Fig. S5B).

One of the critical steps in metastasis that may contribute to these outcomes under the assaying conditions is the extravasation of cancer cells through the blood vessel wall to reach distal organs. To assess the potential function of βig-h3 in extravasation, we used an in vitro TEM assay to test the effect of βig-h3 expression on the TEM capability of colon cancer cells in order to mimic the in vivo behavior of cancer cells undergoing extravasation (Voura et al. 2001). As shown in Figure 4A, SW480 cells were allowed to migrate through a monolayer of human umbilical vein endothelial cells (HUVECs). The TEM process was three times more efficient with βig-h3 overexpression. Consistent with this result, shRNA knockdown of βig-h3 in SW620 cells similarly reduced the ability of those cells to migrate through the HUVEC layer in comparison with the vector control cells (Fig. 4B). Similar results were obtained by using primary human microvascular endothelial cells and immortalized human bone marrow-derived endothelial cells (data not shown), suggesting that the proextravasation function of βig-h3 is not limited to one type of endothelial cell. On the other hand, this effect of βig-h3 is endothelial cell-specific, because the tumor cells with different levels of βig-h3 showed no differences in their ability to migrate through either the fibroblast monolayer or matrigel (Supplemental Fig. S6). These findings provide a potential cellular mechanism (extravasation) for the observed in vivo phenotype of increased formation of metastatic colonies in various organs and tissues of the mice by the colon cancer cells through intravenous or intracardiac inoculation.

It has been established that the permeability of the blood vessel wall is in part controlled by VE-cadherin-dependent junctions between endothelial cells (Vestweber 2002). To intravasate and extravasate the blood vessel, cancer cells often need to acquire the ability to breach the endothelial cell barrier. This process likely occurs through the induction of changes in the organization and integrity of the VE-cadherin junctions, leading to disruption of the interendothelial cell contacts, which in turn allows tumor cells to successfully migrate through (Allport et al. 1997). To examine the capability of βig-h3 to induce changes at the interendothelial cell contacts, fluorescent dye-labeled colon cancer cells with different βig-h3 expression levels were laid on top of the endothelial monolayer, and cells were stained 4 h later with an anti-VE-cadherin antibody to assess the integrity

of the intercellular junctions. The colocalization of fluorescence-labeled cancer cells and VE-cadherin junction disruption (indicated by VE-cadherin immunostaining) was examined using fluorescence microscopy, and the frequency of colocalization was quantified (Sandig et al. 1997). The presence of high-level βig-h3 significantly increased the frequency of VE-cadherin junction disruption in the endothelial monolayer (Fig. 4C,D), which indicates that βig-h3 promotes TEM by facilitating VE-cadherin reorganization and junction dissociation. To further examine the effect of βig-h3 on the integrity of intercellular junctions, we performed a vascular permeability assay (Lampugnani et al. 1992) by treating an intact endothelial monolayer with conditioned media from three types of SW620-derived cells that contain different levels of βig-h3. The permeability of the endothelial monolayer for FITC-coupled dextran was determined at several time points by measuring the fluorescence intensity of the media in the lower compartment. As shown in Figure 4E, the permeability of the endothelial monolayer is proportionally associated with the level of βig-h3 present in the media. These results suggest that βig-h3 enhances extravasation by inducing VE-cadherin junction dissociation, leading to the increase of vascular permeability of the endothelial monolayer.

To determine whether the proextravasation activity of βig-h3 observed under the in vitro assaying conditions is an accurate reflection of its capability in vivo, we monitored the impact of βig-h3 on the ability of colon cancer cells to accumulate in the lungs of mice 24 h after their inoculation via the tail vein as a measure of the extravasation activity following an established protocol (Gupta et al. 2007). As shown in Figure 4, F and G, reduction in βig-h3 expression significantly suppressed the number of cancer cells accumulated in the lung, a strong indication that βig-h3 plays a positive role in the extravasation process during tumor metastasis.

βig-h3-mediated VE-cadherin junction dissociation requires integrin $\alpha_v\beta_5$

As a secreted protein containing multiple integrin-interacting domains, βig-h3 has been shown to interact with various types of integrins, including $\alpha_v\beta_3$, $\alpha_v\beta_5$, $\alpha_3\beta_1$, and $\alpha_6\beta_4$ (Bae et al. 2002; Kim et al. 2003; Nam et al. 2003; Lee et al. 2006). Among them, $\alpha_v\beta_3$ and $\alpha_v\beta_5$ have been demonstrated previously to be associated with the extravasation process (Weerasinghe et al. 1998; Su et al. 2006). As an initial attempt to determine if integrin $\alpha_v\beta_3$ or $\alpha_v\beta_5$ is involved in mediating the activity of βig-h3 in promoting TEM, we pretransfected endothelial cells with an siRNA specifically against integrin α_v to reduce its expression (Supplemental Fig. S7). The TEM activities of the SW480 cancer cells with or without βig-h3 expression through the modified endothelial cell monolayer were assayed 48 h after siRNA transfection. As shown in Figure 5A, knocking down integrin α_v in the endothelial cells reduced the advantage of SW480-βig-h3 cells in their gained TEM activity over the control cells,

Figure 4. βig-h3 promotes cancer cell TEM activity in vitro. (*A,B*) The presence of βig-h3 is associated with increased activity in TEM by colon cancer cells. HUVECs (5×10^4) were plated on the matrigel-coated porous insert in the chambers and maintained overnight in culture to allow the endothelial cells to form a monolayer. Colon cancer cells (1×10^5) labeled with 5-(and-6)-carboxyfluorescein diacetate, succinimidyl ester (CFSE) were then seeded on top of the HUVEC monolayer. After coculturing for 4 h, the cancer cells attached to the bottom of the membrane were fixed for examination under epifluorescence microscope. Each experiment used quadruplicate wells, and within each well counting was done in five randomly selected microscopic high-power fields (200×). Results are the mean ± SD of quadruplicate wells. Four independent experiments were performed. (*) $P < 0.01$ (*n* = 4). (*C*) Monolayers of HUVECs were formed on the matrigel-coated coverslips as described in *A* and *B*. CFSE-labeled colon cancer cells were laid on top of the endothelial monolayer, and samples were taken at 4 h to stain with anti-VE-cadherin antibody (BV9). The colocalization of fluorescent-labeled cancer cells with or without βig-h3 expression and VE-cadherin junction disruption in the endothelial monolayer was examined by fluorescence microscopy. Representative images of the colocalization of tumor cells and VE-cadherin junctions that exhibit either dissociated or intact VE-cadherin junctions are shown. (*D*) Quantification of frequency for the colocalization of SW480 cancer cells with or without βig-h3 expression and VE-cadherin junction dissociation. Each experiment used triplicate coverslips, and within each coverslip 300 CFSE-positive cancer cells were counted. Results are the mean ± SD of three independent experi-

ments. (*) $P < 0.01$ (*n* = 9). (*E*) βig-h3 stimulates permeability in the HUVEC monolayer. A confluent layer of HUVEC cells on Transwell filter inserts was used. Monolayer permeability after addition of indicated conditioned media from SW620-derived cells was measured using FITC-dextran (Mr 40×10^3) as described in the Materials and Methods. Results are the mean ± SD of triplicate wells. Three independent experiments were performed. (*) $P < 0.02$; (**) $P < 0.01$. (*F*) Representative in vivo bioluminescent images of animals at indicated days after intravenous inoculation. Representative mice from SW620-βig-h3n, SW620-VEC, and SW620-βig-h3-shRNA1 groups are shown in the prone position, with relative light unit counts indicated in color. (*G*) SW620-derived cells were injected intravenously, and accumulation of cancer cells in the lung as indication of extravasation activity was measured via bioluminescence on day 1. Results are the mean ± SD of five animals from each group. (*) $P < 0.05$; (**) $P < 0.01$. Two independent experiments were performed.
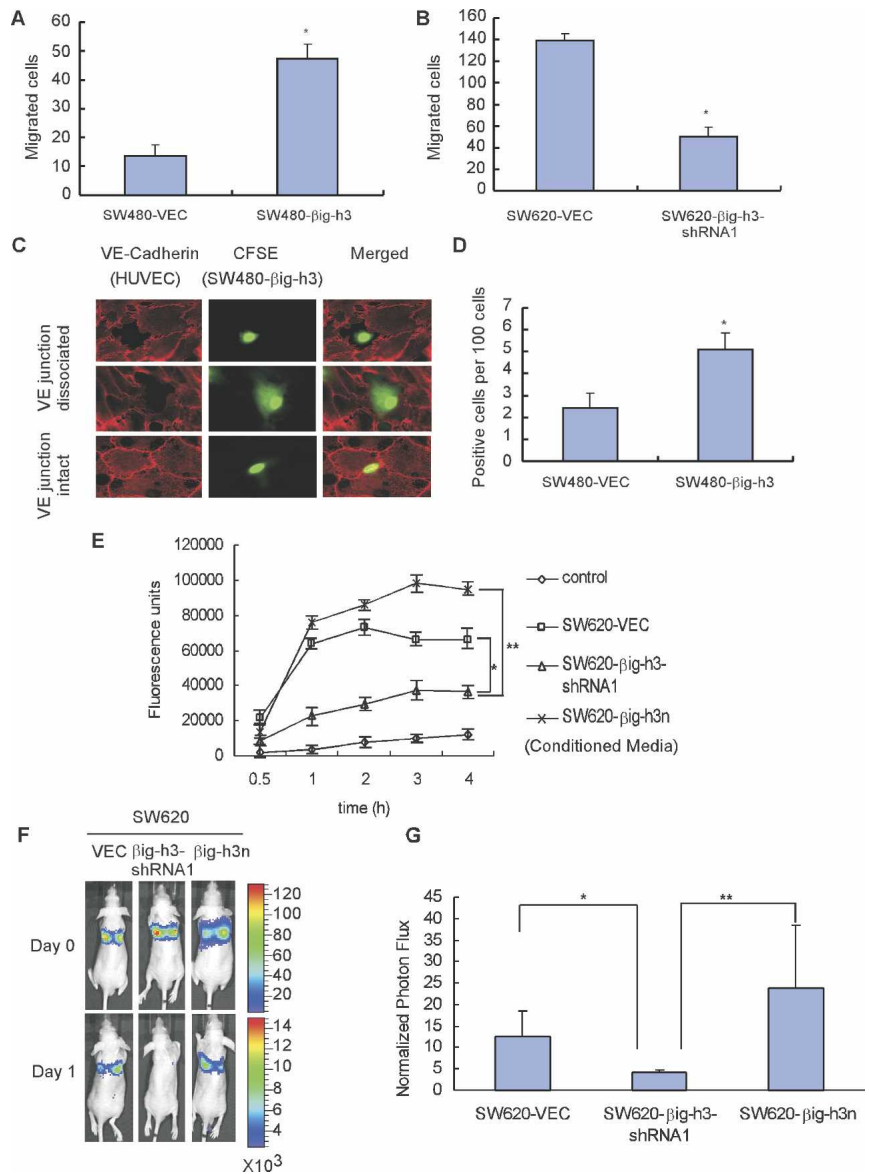
but had a minimal effect on the SW480-VEC control cells. Consistent with these results, reduction of integrin α_v expression in the endothelial cells also significantly blocked the TEM activity of SW620-VEC and SW620-βig-h3n cells (Fig. 5B), suggesting that integrin α_v is involved in βig-h3-mediated enhancement in TEM activity. The specific involvement of integrin $\alpha_v\beta_3$ or $\alpha_v\beta_5$ in this process was subsequently determined by pretreating the endothelial cell monolayer with specific blocking an-

tibodies against integrin $\alpha_v\beta_3$ or $\alpha_v\beta_5$. As shown in Figure 5C, only the antibody against $\alpha_v\beta_5$ abolished the gained TEM activity of the SW480-βig-h3 cells over the control cells. This antibody against integrin $\alpha_v\beta_5$ also eliminated the TEM advantage of SW620-VEC and SW620-βig-h3n cells over the shRNA knockdown cells (Fig. 5D). Collectively, these results indicate that integrin $\alpha_v\beta_5$ is most likely the mediator of βig-h3 activity in promoting TEM.
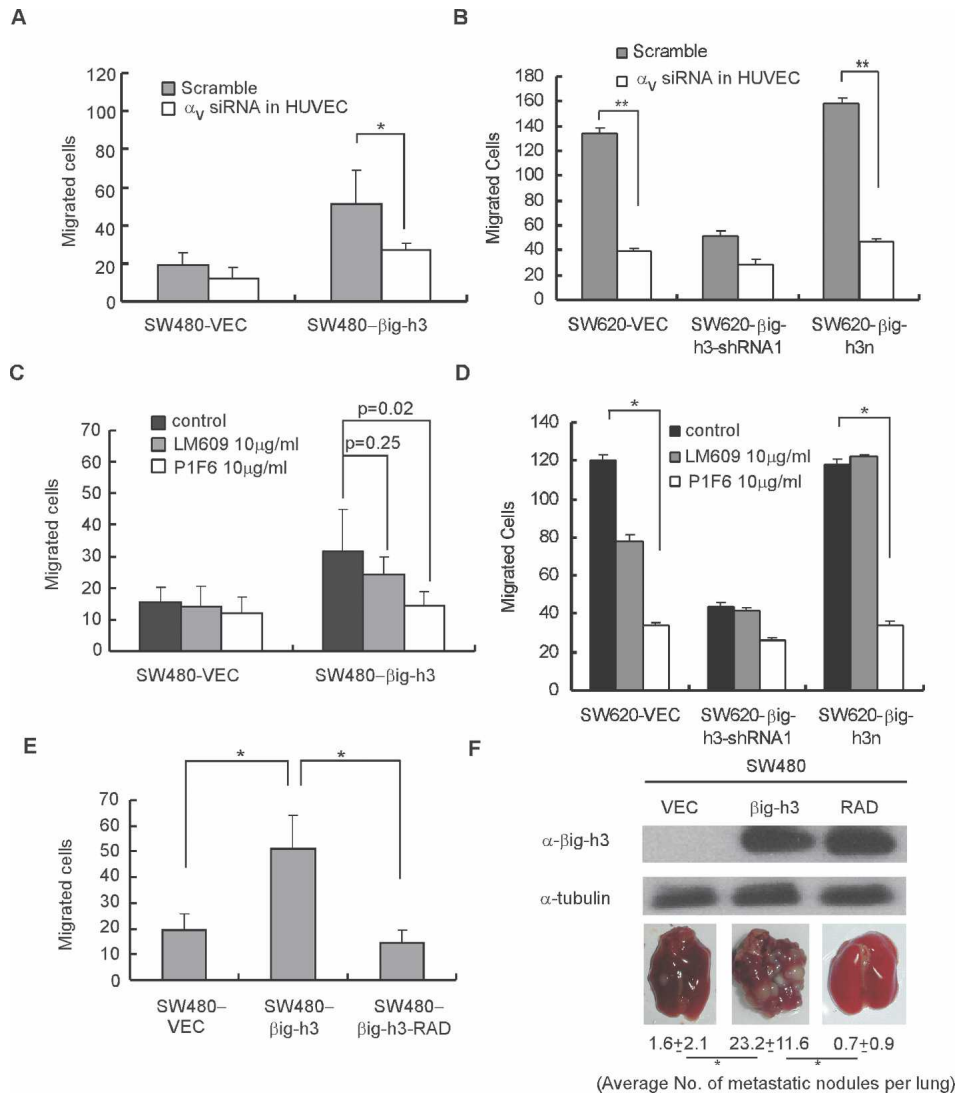
Figure 5. βig-h3-induced TEM is mediated through the $\alpha_v\beta_5$ integrin. (*A,B*) Knockdown of integrin α_v on the surface of HUVECs results in the reduction of βig-h3-induced TEM activity. HUVECs were transfected with control or integrin α_v siRNA 24 h before being plated on the matrigel-coated porous insert. A TEM assay was performed 48 h after siRNA transfection as described in Figure 4. Results are the mean ± SD of quadruplicate wells. Four independent experiments were performed. (*) $P < 0.02$; (**) $P < 0.01$. (*C,D*) The presence of blocking antibody against integrin $\alpha_v\beta_5$ but not $\alpha_v\beta_3$ eliminates βig-h3-induced increase in TEM activity. HUVEC monolayer was pretreated with the indicated concentration of blocking antibody LM609 against integrin $\alpha_v\beta_3$ or P1F6 against integrin $\alpha_v\beta_5$ for 30 min before the CFSE-labeled cancer cells were added and a TEM assay was performed as described earlier. Results are the mean ± SD of quadruplicate wells. Four independent experiments were performed. (*) $P < 0.01$. (*E*) RGD → RAD mutation in βig-h3 abolishes βig-h3-induced increase in TEM activity. TEM assay was performed as described previously with indicated cell lines. Results are the mean ± SD of quadruplicate wells. Four independent experiments were performed; (*) $P < 0.01$. (*F*) SW480 cells (parental) were infected with recombinant retroviruses containing either vector control (VEC), βig-h3 full-length cDNA (βig-h3), or βig-h3-RAD cDNA (RAD). An equal amount of concentrated supernatant from each cell type as indicated was examined for the presence of βig-h3 by Western blot using an anti-βig-h3 antibody. The whole-cell lysate from each sample of cells was blotted with anti-tubulin antibody for loading control. (*Bottom* panel) Representative results showing the formation of metastases in the lung of mice injected with SW480-derived cells. We injected 4×10^6 SW480-VEC, SW480-βig-h3, or SW480-βig-h3-RAD cells through the tail vein into 5-wk-old SCID-Beige mice. Mice were sacrificed and examined for the growth of metastatic tumors 12 wk after injection. The average numbers of metastatic nodules in individual mouse are shown. The counting was performed under a dissection scope. (*) $P < 0.01$ ($n = 10$).

The RGD motif of βig-h3 protein is required for βig-h3-induced TEM

βig-h3 possesses a RGD sequence at its C terminus, which is a known ligand-binding motif for integrins (Delannet et al. 1994). To probe whether the proextravasation activity of βig-h3 is mediated via the RGD motif, a mutant form of βig-h3 was generated by changing RGD to RAD with a glycine-to-alanine substitution. This mutant βig-h3 was introduced into SW480 cells via retrovi-

ral infection to an expression level comparable with that of the wild-type protein (Fig. 5F). As shown in Figure 5E, the RAD mutant of βig-h3 failed to facilitate the TEM of SW480 cells in comparison with wild-type βig-h3. More strikingly, 12 wk after tail vein injection, the SW480-βig-h3-RAD cells barely formed any lung metastases (Fig. 5F). Taken together, these results suggest that the RGD motif in βig-h3 is essential for activating integrin $\alpha_v\beta_5$ to promote TEM and lung metastasis of the colon cancer cells.

To further examine the role of the RGD motif in the βig-h3-stimulated TEM process, we synthesized a blocking peptide corresponding to amino acids 636–655 of βig-h3 containing the RGD motif, and a mutant peptide with the same sequence except for the glycine-to-alanine substitution (Fig. 6A). Vascular permeability assays were performed following pretreatment of the intact endothe-

lial monolayer with the two peptides, respectively. As seen earlier in Figure 4E, βig-h3-conditioned media increased the permeability of the HUVEC monolayer, and this increase was almost completely abolished by preincubation of the HUVEC cells with the blocking peptide (Fig. 6B,C). Note that the RAD peptide had no effect on βig-h3 activity in parallel assays (Fig. 6B,C). These results again suggest that the RGD motif is required for the βig-h3-induced increase in vascular permeability of the endothelial monolayer.

βig-h3 stimulates the activation of Src kinase and tyrosine phosphorylation of β-catenin in endothelial cells

Previous studies have shown that the tyrosine kinase Src serves as an effector downstream from the integrins. Src

Figure 6. βig-h3-induced TEM requires the RGD motif and Src kinase activation. (*A*) Sequences of the RGD and RAD peptides. The numbers represent the positions of the animo acids on the βig-h3 protein. (*B,C*) The RGD peptide blocks the βig-h3-induced permeability in the HUVEC monolayer. Confluent layers of HUVEC cells on Transwell filter inserts were pretreated with each peptide for 1 h at the indicated concentration. Monolayer permeability after addition of conditioned media from SW480- and SW620-derived cells as indicated was measured using FITC-dextran (Mr 40×10^3) as described in the Materials and Methods. Results are the mean ± SD of triplicate wells. Three independent experiments were performed. (*) $P < 0.05$. (*D*) βig-h3-induced TEM activity is associated with the activation of Src kinase in endothelial cells. βig-h3-producing, βig-h3-RAD-producing, or control SW480 cells were grown in normal media until 80% confluency and then cultured in serum-free media for 24 h. Supernatant was collected as conditioned media. HUVEC cells were grown in normal media until 75% confluency and then cultured in serum-free media for 16 h. Conditioned media from βig-h3-producing, βig-h3-RAD-producing, or control SW480 cells were applied to the HUVEC cells, respectively. Cell lysates were harvested at indicated time points and analyzed by immunoblotting with the anti-pY416-Src and anti-Src antibodies. (*E*) Src kinase activation is associated with tyrosine phosphorylation of β-catenin in the endothelial cells. The same type of experiment was performed as described in *D*. Cell lysates harvested at indicated time points were incubated with anti-β-catenin antibody. Immunoprecipitates were blotted with anti-phospho-tyrosine antibody. (*F,G*) Src inhibitor PP1 blocks the βig-h3-induced permeability in the HUVEC monolayer. Confluent layers of HUVEC cells on Transwell filter inserts were pretreated with 170 nM PP1 Src inhibitor for 1 h. Monolayer permeability after addition of conditioned media from the indicated cell types was measured using FITC-dextran (Mr 40×10^3) as described in the Materials and Methods. Results are the mean ± SD of triplicate wells. Three independent experiments were performed. (*) $P < 0.01$.
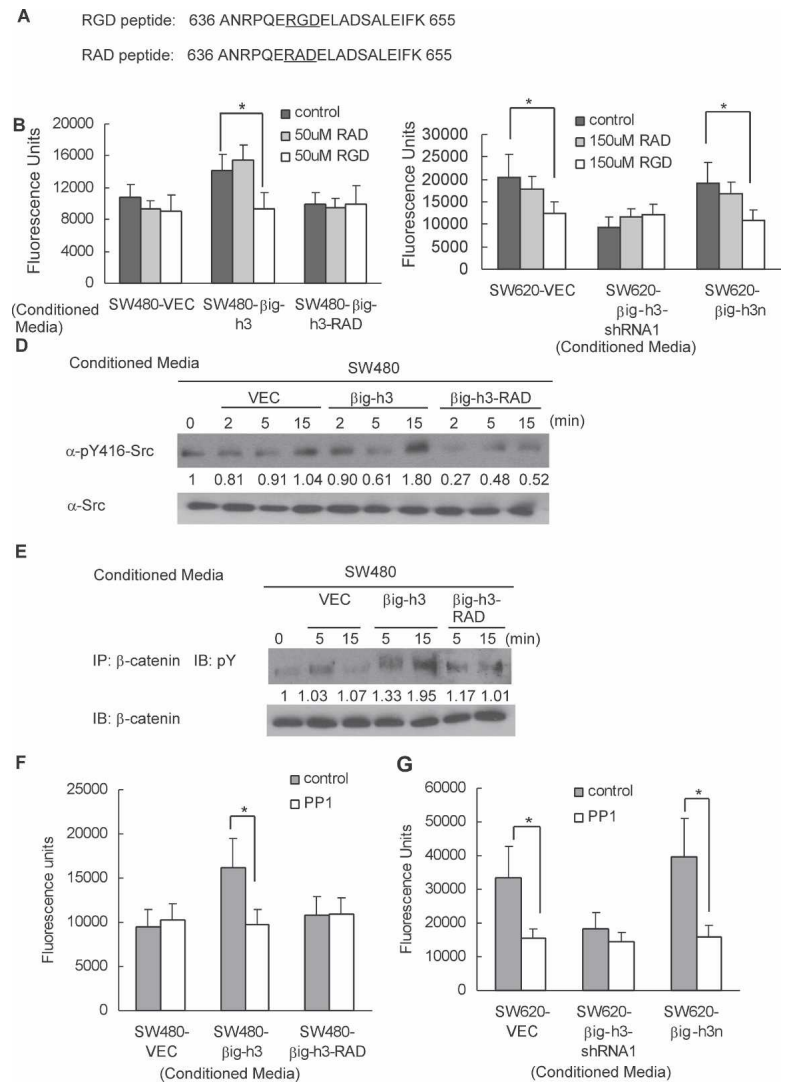
activation results in VE-cadherin and β-catenin phosphorylation on specific tyrosine residues, leading to the dissociation of the VE-cadherin/β-catenin complex and breakdown of the endothelial barrier (Weis et al. 2004). To test if the Src pathway in the endothelial cells mediates βig-h3-induced TEM of cancer cells, we examined Tyr416 phosphorylation of Src, which is indicative of the activated state of the kinase (Hunter 1987). As shown in Figure 6D, a higher level of active Src was detected in the endothelial cells incubated with conditioned media derived from SW480-βig-h3 cells than in those incubated with media from the SW480-VEC and SW480-βig-h3-RAD cells. Moreover, the βig-h3-mediated activation of Src kinase is associated with an enhancement in tyrosine phosphorylation of β-catenin in the endothelial cells (Fig. 6E). On the other hand, blocking Src activity by the kinase inhibitor 4-amino-5-(4-methylphenyl)-7-(t-butyl) pyrazolo [3,4-d]-pyrimidine (PP1) specifically abrogated βig-h3-induced, but not basal-level, TEM activity of the cancer cells (Fig. 6F,G). Taken together, these data strongly suggest that βig-h3-induced TEM is dependent on the $\alpha_v\beta_5$ integrin–Src signaling pathway, the activation of which requires the βig-h3 RGD motif.

Discussion

Several recent reports have highlighted extravasation as a critical step of tumor metastasis that is regulated by various types of secreted or cell surface proteins (Gupta et al. 2007; Karnoub et al. 2007). In one study, four of such proteins expressed by human breast cancer cells were shown to collectively facilitate the breaching of lung capillaries by circulating tumor cells to seed pulmonary metastasis (Gupta et al. 2007). In another study, breast cancer cells were demonstrated to stimulate de novo secretion of the chemokine CCL5 from mesenchymal stem cells, which in turn acts in a paracrine fashion on the cancer cells to enhance the extravasation process (Karnoub et al. 2007). The data presented here demonstrate that the ECM protein βig-h3 promotes colon cancer metastasis primarily at the extravasation step. A low-metastatic colon cancer cell line, SW480, engineered to overexpress βig-h3 displayed a phenotype of greatly enhanced tumor metastasis, whereas down-regulation of βig-h3 in the aggressive isogenic cell line resulted in an almost complete elimination of the metastatic potential when tested in our animal model systems. βig-h3 directly or indirectly interacts with integrin $\alpha_v\beta_5$ on the surface of endothelial cells, and this interaction consequently induces Src activation, which leads to tyrosine phosphorylation of β-catenin, dissociation of VE-cadherin junction, and eventual breakdown of the endothelial barrier. The integrin $\alpha_v\beta_5$ and the Src signal pathway have both been implicated in the extravasation process (Weis et al. 2004; Su et al. 2006). The establishment of an association between βig-h3 and the integrin $\alpha_v\beta_5$–Src signaling pathway thus provides a molecular mechanism for the novel proextravasation role of βig-h3 in the context of colon cancer metastasis.

In addition to colon cancer, βig-h3 up-regulation is also observed in cancers of other organs such as pancreas (Schneider et al. 2002). Although the potential function of βig-h3 in pancreatic cancers is not known, the aberrant expression of βig-h3 may contribute to the pathologic phenotype of the disease in a similar way as in colon cancer. Intriguingly, besides the changes of βig-h3 expression in epithelial cancer cells, aberrant expression of βig-h3 is also found in cancer-associated fibroblasts/myofibroblasts, including colon and breast cancers (Buckhaults et al. 2001; Allinen et al. 2004; data not shown). The tumor microenvironment may extensively influence gene expressions in the cancer-associated fibroblasts, which in turn secrete growth factors and/or ECM proteins (such as βig-h3) that react on the tumor microenvironment (Bhowmick et al. 2004; Mueller and Fusenig 2004; Grum-Schwensen et al. 2005; Orimo et al. 2005; Orimo and Weinberg 2006). It is important to note that, unlike a bone fide growth factor or oncoprotein that stimulates cell proliferation, βig-h3 showed no mitogenic activity on cancer cells under in vitro assaying conditions (Supplemental Fig. S5B; data not shown). Rather, this ECM protein acts in vivo to promote metastasis by altering the tumor microenvironment.

As the nomenclature implies, βig-h3 was originally identified as a TGF-β-inducible gene (Skonier et al. 1992). Since TGF-β has been implicated in promoting tumor metastasis (Kang et al. 2005; Bierie and Moses 2006; Gomis et al. 2006), it is possible that βig-h3 acts as an effector in mediating the prometastatic activity of TGF-β in certain cancers. A recent study on breast tumor heterogeneity (Shipitsin et al. 2007) showed that cells in breast tumors can be categorized according to CD44^{+} and CD24^{+} expression. Tumors consisting of cells with high CD44^{+}:CD24^{+} ratios tend to develop distant metastases, particularly to the bone (Shipitsin et al. 2007). Gene expression profile analyses of these cells show that TGF-β signaling and βig-h3 expression are specifically up-regulated in the CD44^{+} cells, indicating a potential role of TGF-β signaling in tumor metastasis and a potential link between TGF-β action and βig-h3 expression in CD44^{+} breast cancer cells.

In previous studies, we identified periostin, a structural homolog of βig-h3, as a positive regulator of colon cancer progression. Periostin potently promotes colon cancer metastasis by augmenting cell survival via the integrin–Akt/PKB pathway (Bao et al. 2004). Interestingly, although periostin and βig-h3 share significant sequence and structural homology (Supplemental Fig. S1), these two proteins are involved in different processes during tumor development, which is likely due to the differences in their C-terminal structure. βig-h3 has a short C terminus that contains a RGD motif, while periostin possesses a relatively long hydrophilic C terminus without the RGD sequence. The differences in their C termini may contribute to their differential binding specificities with different types of integrins, which in turn result in diverse impacts on tumor progression. It is intriguing that the βig-h3-RAD mutant apparently exerted a dominant-negative effect on the formation of lung metastasis by the SW480 cells (Fig. 5F), suggesting

that other molecules that possess similar activities as βig-h3 may also be involved in the metastatic process. In addition, we found that a small βig-h3-derived peptide effectively blocked the TEM of cancer cells, indicating an intriguing possibility that βig-h3 can be a potential therapeutic target for treating metastatic colon cancer.

Materials and methods

Immunohistochemical staining

Paraffin-embedded lung tissue sections from mice inoculated with SW480-βig-h3 or SW480-VEC cancer cells or TMA slides were processed for antigen retrieval by heating in 10 mM sodium citrate (pH 6.0) for 20 min at 95°C. Then, sections were immunostained with a polyclonal antibody against the recombinant human βig-h3 protein (Proteintech Group, Inc., catalog no. 10188-1-AP). The immunostaining was performed with an ABC staining system (Vector Laboratories) using the avidin-biotinylated-peroxidase detection method.

Criteria for TMA evaluation

Immunoreactivity of βig-h3 was semiquantitatively examined by a pathologist (M. Datto) as described previously (Reed et al. 2002). For each tumor, represented by TMA staining, we determined the tumor epithelial cells' proportion score and intensity score. Peritumoral inflammatory and stromal cells were not included in the evaluation. The proportion score included the fraction of positively stained tumor cells and was as follows: 0 (0%), 1 (1%–33%), 2 (34%–66%); 3 (67%–100%). The positive reaction is scored into four grades, according to the intensity of the staining as follows: 0; 1 +; 2 +; 3 +. The product of the intensity by percentage scores is used as the final score. For the statistical analysis, a score of 0 was considered negative, a score of 1–3 was considered weak, a score of 4–6 was considered moderate, and a score of 7–9 was considered strong.

Statistical analysis

The immunohistochemical staining results were analyzed by using the ANOVA F test. A pairwise comparison was done between different tumor grades.

Plasmids

A cDNA sequence encoding Flag epitope-tagged βig-h3 was cloned into the SnaBI/SalI sites of pBabe-puro (Morgenstern and Land 1990) to generate pBabe-βig-h3-Flag-puro. Retroviral vectors that encode shRNAs against the βig-h3 transcript were generated by cloning oligonucleotide sequences into the pSUPER-retro-puro (Brummelkamp et al. 2002) vector. The coding sequences of the βig-h3 targeting shRNAs were CCAGCTGGC CTCTAAGTAT (βig-h3-shRNA1) and CACGATGCTTGAAG GTAAC (βig-h3-shRNA2). shRNA-resistant mutations were generated by site-directed mutagenesis in the coding sequence of Ala445 (GCC → GCA) and Ser446 (TCT → TCG) to create an shRNA-resistant version of the βig-h3 expression plasmid pBabe-βig-h3n-Flag-neo. pMCVS-luciferase was a generous gift from Dr. P. Casey of Duke University.

Cell culture and transfection

SW480/SW620 and their various derivatives of cell populations, as well as 293T cells, were cultured in DMEM growth medium (Invitrogen Corp.) supplemented with 10% FBS and antibiotics. The HUVECs and human microvascular endothelial cells (HMVECs; Clonetics) were maintained in endothelial growth medium (EGM-2-MV; Clonetics) supplemented with 5% FBS (Clonetics). The human bone marrow-derived endothelial cells (HBMEC-28 and HBMEC-60) were maintained in M199 (Invitrogen Corp.) supplemented with 10% FBS and 10% heat-inactive human serum (Sigma) as described previously (Schweitzer et al. 1995). Retroviruses expressing βig-h3 shRNA, βig-h3-Flag-puro, βig-h3n-Flag-neo, or luciferase were produced from the 293T packaging cell line. 293T cell transfections were performed using FuGene 6 reagent (Roche) according to the manufacturer's instructions. Viruses were harvested 48 and 72 h after transfection, filtered, and used to infect SW480 or SW620 cell cultures in the presence of 5 µg/mL polybrene. Infected cells were selected for puromycin or G418 resistance.

Subcutaneous injection Cancer cells were harvested from subconfluent cell culture plates, washed with PBS, and resuspended at a concentration of $2.5 × 10^7$ cells per milliliter of DMEM with 10% FBS. Of the suspending cells, 0.2 mL was injected into 5-wk-old SCID-Beige mice (Charles River Laboratories) with five mice for each group. Twelve weeks after injection, mice were sacrificed and examined for the growth of subcutaneous tumors. Four independent experiments were performed.

Intravenous injection Cancer cells were harvested at a concentration of $2 × 10^7$ cells per milliliter of DMEM with 10% FBS. Of the suspending cells, 0.2 mL was injected through the tail vein into 5-wk-old SCID-Beige mice using 30-gauge needles with five mice for each group. Mice were sacrificed and examined for the growth of metastatic tumors at various time points. Mice injected with SW480-βig-h3 or SW480-VEC cells were sacrificed 12 wk after injection. Mice injected with SW620-VEC or SW620-βig-h3-shRNA cells were sacrificed 7 wk after injection. Mice injected with SW620-βig-h3n cells were sacrificed 4 wk after injection. Four independent experiments were performed for each pair of cancer cells.

Intracardiac injections Cells were harvested at a concentration of $1 × 10^7$ cells per milliliter of PBS. We injected $1 × 10^6$ into the left cardiac ventricle of 5-wk-old, female BALB/c-nu/nu nude mice (National Cancer Institute) using 27-gauge needles (Yin et al. 1999). Mice were anesthetized with 2.5% avertin (20 mL per 1 kg of body weight) before injection. A successful injection was indicated by the pumping of arterial blood into the syringe and confirmed by immediate bioluminescence imaging. All animals were maintained in a specific pathogen-free facility, and all studies were conducted under protocols approved by the Duke University Institutional Animal Care and Use Committee.

Bioluminescence imaging

Animals were injected with 10 mg/kg D-luciferin (Xenogen) in PBS intraperitoneally and anesthetized by isofluorane using the XGI-8 gas anesthesia system (Xenogen). Bioluminescence images were acquired by using the IVIS Imaging System (Xenogen) 10–15 min after injection. The acquisition time was 60 sec.

Western blot analysis, immunoprecipitation, and antibodies

For the detection of secreted βig-h3 protein, βig-h3-producing or control cells were grown in normal media until 80% confluency and then cultured in serum-free media for 24 h. The serum-free

conditioned media were collected and analyzed by immunoblot with a specific anti-βig-h3 polyclonal antibody (Proteintech Group, Inc.), anti-Flag antibody (Sigma). As a loading control, whole-cell lysates were blotted with anti-γ-tubulin antibody (Sigma). For the detection of Src and other proteins, cell lysates were analyzed by immunoblotting with the anti-SRC (src-2; Santa Cruz Biotechnology, Inc.) and anti-pY416-SRC (Cell Signaling Technology, Inc.) rabbit polyclonal antibodies. To examine the tyrosine phosphorylation of β-catenin, HUVEC cells stimulated with conditioned media were harvested with RIPA lysis buffer (50 mM Tris-HCl at pH 7.4, 150 mM NaCl, 1% Triton X-100, 1% sodium deoxycholate, 0.1% SDS) supplemented with protease inhibitors (20 μg/mL leupeptin, 10 μg/mL pepstatin A, 10 μg/mL aprotonin, 1 mM PMSF) and phosphatase inhibitors (10 mM sodium orthovanadate, 10 mM sodium fluoride). The cleared lysates were immunoprecipitated with anti-β-catenin antibody (E5; Santa Cruz Biotechnology, Inc.) and protein A/G-Sepharose. The immunoprecipitates were washed three times with lysis buffer, solubilized with SDS-PAGE sample buffer, electrophoresed, and analyzed by immunoblotting with anti-phospho-tyrosine antibody (4G10; Millipore). Anti-$\alpha_v\beta_3$ mAb (LM609; Chemicon, Inc.) and anti-$\alpha_v\beta_5$ mAb (P1F6; Chemicon) were used at 10 μg/mL for the functional blocking experiments. Quantification of results was aided by the ImageJ software (W.S. Rasband, U.S. National Institutes of Health; http://rsb.info.nih.gov/ij, 1997–2006).

TEM assay

HUVECs (5×10^4) were plated on the matrigel-coated porous insert in the chambers and maintained overnight in conditioned media to allow the endothelial cells to form a monolayer as described previously (Tremblay et al. 2006). Colon cancer cells (1×10^5) in suspension were labeled for 10 min with 5-(and-6)-carboxyfluorescein diacetate, succinimidyl ester (CFSE; Molecular Probes) at 37°C and washed three times with PBS containing 5% FBS. Cancer cells were then seeded on top of the HUVEC monolayer. After coculturing for 4 h, the cancer cells attached to the bottom of the membrane were fixed for examination by epifluorescence microscopy. Each experiment used quadruplicate wells, and within each well counting was done in five randomly selected microscopic high-power fields (200×). Four independent experiments were performed. The same assay was repeated using HMVECs or HBMECs plated in monolayers in replacement of HUVECs.

siRNA transfection

HUVECs or HMVECs were grown to 75% confluency in six-well culture plates. Scramble or Integrin α_v siRNA (Graef et al. 2005) (Dharmacon) were transfected with Lipofectamine 2000 (Invitrogen Corp.) according to the manufacturer's instructions. After 6 h of incubation, fresh medium was added to the cells. Forty-eight hours after transfection, TEM and FACS analysis were performed.

Immunofluorescence microscopy

Monolayer HUVECs were incubated with an anti-VE-cadherin antibody, BV9 (Abcam; 1:20 in EGM-2 medium) for 20 min at room temperature and washed with PBS three times. Cells were then fixed with 4% paraformaldehyde followed by PBS washes. After blocking with 2.5% normal goat serum, cells were incubated with secondary antibody for 45 min. Following three PBS washes, the cells were stained with Hoechst (Sigma). Samples were visualized on a Zeiss LSM410 confocal microscope.

Vascular permeability assay

HUVEC cells (2.7×10^4) were seeded on fibronectin-coated Transwell filters (0.4-μm pore size; Costar) in 24-well plates and cultured with 100 μL of EGM-2 media in the upper chamber and 600 μL in the lower chamber. The cells were grown for 3 d without medium change until they had reached confluence. For the assay, 100 μL of the indicated conditioned media with 4 μL of FITC-dextran (Mr 4×10^4; Sigma; final concentration 1 mg/mL) were added to the upper chamber. At the indicated time points, 50-μL samples were taken from the lower chamber and replaced immediately with the same volume of growth medium to maintain hydrostatic equilibrium. The samples were diluted to 1 mL with PBS, and the fluorescent content was measured at 492/520 nm absorption/emission wavelengths for FITC-dextran. For the peptide blockade and Src inhibitor pretreatment assays, the endothelial monolayer was pretreated with peptides or Src inhibitor PP1 at the indicated concentration for 1 h before FITC-dextran and conditioned media were added. The fluorescent content in the lower chamber was measured 4 h later.

Cell survival assay under hypoxia condition

βig-h3-producing and vector-control SW480 cells were grown in the normal media until 60%–70% confluency. Then, they were treated with 100 μM DFO (Deferoxamine; Sigma) to mimic hypoxia (Bianchi et al. 1999) for different time points as indicated, and the numbers of surviving cells at different time points were analyzed and counted. The results were quantified from three independent experiments.

Anoikis assay

To determine the effect of βig-h3 on cell survival under an anoikis-inducing condition, cells were prevented from adhering by culturing them in Petri dishes coated with PolyHema (Sigma) as described previously (Bao et al. 2004). Subconfluent βig-h3-producing or the vector-control SW480 cells were trypsinized, washed, and transferred to the PolyHema-coated Petri dishes in the serum-free media and then incubated for different time points as indicated. Apoptotic cells from PolyHema-coated dishes were checked and analyzed using the Annexin V Apoptosis Detection Kit (BD Pharmingen).

Acknowledgments

References

Allinen, M., Beroukhim, R., Cai, L., Brennan, C., Lahti-Domenici, J., Huang, H., Porter, D., Hu, M., Chin, L., Richardson, A., et al. 2004. Molecular characterization of the tumor microenvironment in breast cancer. *Cancer Cell* **6:** 17–32.

Allport, J.R., Ding, H., Collins, T., Gerritsen, M.E., and Luscinskas, F.W. 1997. Endothelial-dependent mechanisms regulate leukocyte transmigration: A process involving the proteasome and disruption of the vascular endothelial–cadherin complex at endothelial cell-to-cell junctions. *J. Exp. Med.* **186:** 517–527.

Argani, P., Rosty, C., Reiter, R.E., Wilentz, R.E., Murugesan, S.R., Leach, S.D., Ryu, B., Skinner, H.G., Goggins, M., Jaffee,

E.M., et al. 2001. Discovery of new markers of cancer through serial analysis of gene expression: Prostate stem cell antigen is overexpressed in pancreatic adenocarcinoma. *Cancer Res.* **61:** 4320–4324.

Bae, J.S., Lee, S.H., Kim, J.E., Choi, J.Y., Park, R.W., Yong Park, J., Park, H.S., Sohn, Y.S., Lee, D.S., Bae Lee, E., et al. 2002. βig-h3 supports keratinocyte adhesion, migration, and proliferation through α3β1 integrin. *Biochem. Biophys. Res. Commun.* **294:** 940–948.

Bao, S., Ouyang, G., Bai, X., Huang, Z., Ma, C., Liu, M., Shao, R., Anderson, R.M., Rich, J.N., and Wang, X.F. 2004. Periostin potently promotes metastatic growth of colon cancer by augmenting cell survival via the Akt/PKB pathway. *Cancer Cell* **5:** 329–339.

Bastiani, M.J., Harrelson, A.L., Snow, P.M., and Goodman, C.S. 1987. Expression of fasciclin I and II glycoproteins on subsets of axon pathways during neuronal development in the grasshopper. *Cell* **48:** 745–755.

Bernstein, L.R. and Liotta, L.A. 1994. Molecular mediators of interactions with extracellular matrix components in metastasis and angiogenesis. *Curr. Opin. Oncol.* **6:** 106–113.

Bhowmick, N.A., Neilson, E.G., and Moses, H.L. 2004. Stromal fibroblasts in cancer initiation and progression. *Nature* **432:** 332–337.

Bianchi, L., Tacchini, L., and Cairo, G. 1999. HIF-1-mediated activation of transferrin receptor gene transcription by iron chelation. *Nucleic Acids Res.* **27:** 4223–4227.

Bierie, B. and Moses, H.L. 2006. Tumour microenvironment: TGFβ: The molecular Jekyll and Hyde of cancer. *Nat. Rev. Cancer* **6:** 506–520.

Brummelkamp, T.R., Bernards, R., and Agami, R. 2002. Stable suppression of tumorigenicity by virus-mediated RNA interference. *Cancer Cell* **2:** 243–247.

Buckhaults, P., Rago, C., St Croix, B., Romans, K.E., Saha, S., Zhang, L., Vogelstein, B., and Kinzler, K.W. 2001. Secreted and cell surface genes expressed in benign and malignant colorectal tumors. *Cancer Res.* **61:** 6996–7001.

Chambers, A.F., Groom, A.C., and MacDonald, I.C. 2002. Dissemination and growth of cancer cells in metastatic sites. *Nat. Rev. Cancer* **2:** 563–572.

Cooper, C.R., Chay, C.H., Gendernalik, J.D., Lee, H.L., Bhatia, J., Taichman, R.S., McCauley, L.K., Keller, E.T., and Pienta, K.J. 2003. Stromal factors involved in prostate carcinoma metastasis to bone. *Cancer* **97 (Suppl. 3):** 739–747.

Delannet, M., Martin, F., Bossy, B., Cheresh, D.A., Reichardt, L.F., and Duband, J.L. 1994. Specific roles of the $\alpha_V\beta_1$, $\alpha_V\beta_3$ and $\alpha_V\beta_5$ integrins in avian neural crest cell adhesion and migration on vitronectin. *Development* **120:** 2687–2702.

Ferguson, J.W., Thoma, B.S., Mikesh, M.F., Kramer, R.H., Bennett, K.L., Purchio, A., Bellard, B.J., and LeBaron, R.G. 2003. The extracellular matrix protein βIG-H3 is expressed at myotendinous junctions and supports muscle cell adhesion. *Cell Tissue Res.* **313:** 93–105.

Gomis, R.R., Alarcon, C., Nadal, C., Van Poznak, C., and Massague, J. 2006. C/EBPβ at the core of the TGFβ cytostatic response and its evasion in metastatic breast cancer cells. *Cancer Cell* **10:** 203–214.

Graef, T., Steidl, U., Nedbal, W., Rohr, U., Fenk, R., Haas, R., and Kronenwett, R. 2005. Use of RNA interference to inhibit integrin subunit α_V-mediated angiogenesis. *Angiogenesis* **8:** 361–372.

Grum-Schwensen, B., Klingelhofer, J., Berg, C.H., El-Naaman, C., Grigorian, M., Lukanidin, E., and Ambartsumian, N. 2005. Suppression of tumor development and metastasis formation in mice lacking the S100A4(mts1) gene. *Cancer Res.* **65:** 3772–3780.

Gupta, G.P., Nguyen, D.X., Chiang, A.C., Bos, P.D., Kim, J.Y., Nadal, C., Gomis, R.R., Manova-Todorova, K., and Massague, J. 2007. Mediators of vascular remodelling co-opted for sequential steps in lung metastasis. *Nature* **446:** 765–770.

Hanahan, D. and Weinberg, R.A. 2000. The hallmarks of cancer. *Cell* **100:** 57–70.

Hewitt, R.E., McMarlin, A., Kleiner, D., Wersto, R., Martin, P., Tsokos, M., Stamp, G.W., and Stetler-Stevenson, W.G. 2000. Validation of a model of colon cancer progression. *J. Pathol.* **192:** 446–454.

Horiuchi, K., Amizuka, N., Takeshita, S., Takamatsu, H., Katsuura, M., Ozawa, H., Toyama, Y., Bonewald, L.F., and Kudo, A. 1999. Identification and characterization of a novel protein, periostin, with restricted expression to periosteum and periodontal ligament and increased expression by transforming growth factor β. *J. Bone Miner. Res.* **14:** 1239–1249.

Hunter, T. 1987. A tail of two src's: Mutatis mutandis. *Cell* **49:** 1–4.

Kang, Y., He, W., Tulley, S., Gupta, G.P., Serganova, I., Chen, C.R., Manova-Todorova, K., Blasberg, R., Gerald, W.L., and Massague, J. 2005. Breast cancer bone metastasis mediated by the Smad tumor suppressor pathway. *Proc. Natl. Acad. Sci.* **102:** 13909–13914.

Karnoub, A.E., Dash, A.B., Vo, A.P., Sullivan, A., Brooks, M.W., Bell, G.W., Richardson, A.L., Polyak, K., Tubo, R., and Weinberg, R.A. 2007. Mesenchymal stem cells within tumour stroma promote breast cancer metastasis. *Nature* **449:** 557–563.

Kim, M.O., Yun, S.J., Kim, I.S., Sohn, S., and Lee, E.H. 2003. Transforming growth factor-β-inducible gene-h3 (β(ig)-h3) promotes cell adhesion of human astrocytoma cells in vitro: Implication of α6β4 integrin. *Neurosci. Lett.* **336:** 93–96.

Lampugnani, M.G., Resnati, M., Raiteri, M., Pigott, R., Pisacane, A., Houen, G., Ruco, L.P., and Dejana, E. 1992. A novel endothelial-specific membrane protein is a marker of cell–cell contacts. *J. Cell Biol.* **118:** 1511–1522.

LeBaron, R.G., Bezverkov, K.I., Zimber, M.P., Pavelec, R., Skonier, J., and Purchio, A.F. 1995. β IG-H3, a novel secretory protein inducible by transforming growth factor-β, is present in normal skin and promotes the adhesion and spreading of dermal fibroblasts in vitro. *J. Invest. Dermatol.* **104:** 844–849.

Lee, B.H., Bae, J.S., Park, R.W., Kim, J.E., Park, J.Y., and Kim, I.S. 2006. βig-h3 triggers signaling pathways mediating adhesion and migration of vascular smooth muscle cells through αvβ5 integrin. *Exp. Mol. Med.* **38:** 153–161.

Leibovitz, A., Stinson, J.C., McCombs III, W.B., McCoy, C.E., Mazur, K.C., and Mabry, N.D. 1976. Classification of human colorectal adenocarcinoma cell lines. *Cancer Res.* **36:** 4562–4569.

MacDonald, I.C., Groom, A.C., and Chambers, A.F. 2002. Cancer spread and micrometastasis development: Quantitative approaches for in vivo models. *Bioessays* **24:** 885–893.

Morgenstern, J.P. and Land, H. 1990. Advanced mammalian gene transfer: High titre retroviral vectors with multiple drug selection markers and a complementary helper-free packaging cell line. *Nucleic Acids Res.* **18:** 3587–3596.

Mueller, M.M. and Fusenig, N.E. 2004. Friends or foes—Bipolar effects of the tumour stroma in cancer. *Nat. Rev. Cancer* **4:** 839–849.

Nam, J.O., Kim, J.E., Jeong, H.W., Lee, S.J., Lee, B.H., Choi, J.Y., Park, R.W., Park, J.Y., and Kim, I.S. 2003. Identification of the αvβ3 integrin-interacting motif of βig-h3 and its anti-angiogenic effect. *J. Biol. Chem.* **278:** 25902–25909.

O'Brien, E.R., Bennett, K.L., Garvin, M.R., Zderic, T.W., Hinohara, T., Simpson, J.B., Kimura, T., Nobuyoshi, M., Mizgala,

H., Purchio, A., et al. 1996. βig-h3, a transforming growth factor-β-inducible gene, is overexpressed in atherosclerotic and restenotic human vascular lesions. *Arterioscler. Thromb. Vasc. Biol.* **16:** 576–584.

Orimo, A. and Weinberg, R.A. 2006. Stromal fibroblasts in cancer: A novel tumor-promoting cell type. *Cell Cycle* **5:** 1597–1601.

Orimo, A., Gupta, P.B., Sgroi, D.C., Arenzana-Seisdedos, F., Delaunay, T., Naeem, R., Carey, V.J., Richardson, A.L., and Weinberg, R.A. 2005. Stromal fibroblasts present in invasive human breast carcinomas promote tumor growth and angiogenesis through elevated SDF-1/CXCL12 secretion. *Cell* **121:** 335–348.

Reed, J., Ouban, A., Schickor, F.K., Muraca, P., Yeatman, T., and Coppola, D. 2002. Immunohistochemical staining for c-Kit (CD117) is a rare event in human colorectal carcinoma. *Clin. Colorectal Cancer* **2:** 119–122.

Sandig, M., Voura, E.B., Kalnins, V.I., and Siu, C.H. 1997. Role of cadherins in the transendothelial migration of melanoma cells in culture. *Cell Motil. Cytoskeleton* **38:** 351–364.

Schneider, D., Kleeff, J., Berberat, P.O., Zhu, Z., Korc, M., Friess, H., and Buchler, M.W. 2002. Induction and expression of βig-h3 in pancreatic cancer cells. *Biochim. Biophys. Acta* **1588:** 1–6.

Schweitzer, C.M., van der Schoot, C.E., Drager, A.M., van der Valk, P., Zevenbergen, A., Hooibrink, B., Westra, A.H., and Langenhuijsen, M.M. 1995. Isolation and culture of human bone marrow endothelial cells. *Exp. Hematol.* **23:** 41–48.

Shao, R., Bao, S., Bai, X., Blanchette, C., Anderson, R.M., Dang, T., Gishizky, M.L., Marks, J.R., and Wang, X.F. 2004. Acquired expression of periostin by human breast cancers promotes tumor angiogenesis through up-regulation of vascular endothelial growth factor receptor 2 expression. *Mol. Cell. Biol.* **24:** 3992–4003.

Shipitsin, M., Campbell, L.L., Argani, P., Weremowicz, S., Bloushtain-Qimron, N., Yao, J., Nikolskaya, T., Serebryiskaya, T., Beroukhim, R., Hu, M., et al. 2007. Molecular definition of breast tumor heterogeneity. *Cancer Cell* **11:** 259–273.

Skonier, J., Neubauer, M., Madisen, L., Bennett, K., Plowman, G.D., and Purchio, A.F. 1992. cDNA cloning and sequence analysis of βig-h3, a novel gene induced in a human adenocarcinoma cell line after treatment with transforming growth factor-β. *DNA Cell Biol.* **11:** 511–522.

Su, G., Hodnett, M., Wu, N., Atakilit, A., Kosinski, C., Godzich, M., Huang, X.Z., Kim, J.K., Frank, J.A., Matthay, M.A., et al. 2006. Integrin $\alpha_v\beta_5$ regulates lung vascular permeability and pulmonary endothelial barrier function. *Am. J. Respir. Cell Mol. Biol.* **10:** 10–11.

Tremblay, P.L., Auger, F.A., and Huot, J. 2006. Regulation of transendothelial migration of colon cancer cells by E-selectin-mediated activation of p38 and ERK MAP kinases. *Oncogene* **25:** 6563–6573.

Vestweber, D. 2002. Regulation of endothelial cell contacts during leukocyte extravasation. *Curr. Opin. Cell Biol.* **14:** 587–593.

Voura, E.B., Ramjeesingh, R.A., Montgomery, A.M., and Siu, C.H. 2001. Involvement of integrin $\alpha_v\beta_3$ and cell adhesion molecule L1 in transendothelial migration of melanoma cells. *Mol. Biol. Cell* **12:** 2699–2710.

Weerasinghe, D., McHugh, K.P., Ross, F.P., Brown, E.J., Gisler, R.H., and Imhof, B.A. 1998. A role for the $\alpha_v\beta_3$ integrin in the transmigration of monocytes. *J. Cell Biol.* **142:** 595–607.

Weis, S.M. and Cheresh, D.A. 2005. Pathophysiological consequences of VEGF-induced vascular permeability. *Nature* **437:** 497–504.

Weis, S., Cui, J., Barnes, L., and Cheresh, D. 2004. Endothelial barrier disruption by VEGF-mediated Src activity potentiates tumor cell extravasation and metastasis. *J. Cell Biol.* **167:** 223–229.

Weiss, L. 1990. Metastatic inefficiency. *Adv. Cancer Res.* **54:** 159–211.

Woodhouse, E.C., Chuaqui, R.F., and Liotta, L.A. 1997. General mechanisms of metastasis. *Cancer* **80 (Suppl. 8):** 1529–1537.

Yin, J.J., Selander, K., Chirgwin, J.M., Dallas, M., Grubbs, B.G., Wieser, R., Massague, J., Mundy, G.R., and Guise, T.A. 1999. TGF-β signaling blockade inhibits PTHrP secretion by breast cancer cells and bone metastases development. *J. Clin. Invest.* **103:** 197–206.

Zhang, L., Zhou, W., Velculescu, V.E., Kern, S.E., Hruban, R.H., Hamilton, S.R., Vogelstein, B., and Kinzler, K.W. 1997. Gene expression profiles in normal and cancer cells. *Science* **276:** 1268–1272.